Asian Journal of Chemistry; Vol. 36, No. 4 (2024), 974-982

ASIAN JOURNAL OF CHEMISTRY

https://doi.org/10.14233/ajchem.2024.31029

Adsorptive Removal of Methylene Blue Dye by Annealed Waste Foundry Sand

Chandrashekhar R. Patil[1], Suryakant A. Patil[2], Anita K. Tawade[3], Bhagyashri B. Kambale[4], Shivaji N. Tayade[4], Sharad S. Patil[5] and Dnyandev N. Zambare[1,*]

[1]Department of Chemistry, Kisanveer Mahavidyalaya, Wai-412803, India
[2]School of Forensic Science, National Forensic Sciences University, Goa Campus, Ponda-403401, India
[3]Department of Nanoscience, Shivaji University, Kolhapur-416004, India
[4]Department of Chemistry, Shivaji University, Kolhapur-411 004, India
[5]Department of Physics, Shivaji University, Kolhapur-416004, India

*Corresponding author: E-mail: dnzambare123@gmail.com

Received: 8 December 2023; *Accepted*: 19 March 2024; *Published online*: 30 March 2024; AJC-21600

Under optimized experimental conditions, the efficient removal of methylene blue dye from annealed waste foundry sand as adsorbent was carried out. The X-ray diffraction (XRD), X-ray photoelectron spectroscopy (XPS), Field emission scanning electron microscopy (FE-SEM) and partical size analysis were used to confirm the crystalline structure, composition and morphology of the prepared sorbent. The sorbent achieved its highest adsorption capacity by interacting with an aqueous solution contaminated with methylene blue dye. A comparison was made between the sorbent and three annealed sands based on their dye removal efficiency adsorption data over time. By using Langmuir and pseudo second-order kinetic models to the sorption data, it is observed that both physical and chemical processes can influence the removal process. According to experimental data, annealed waste foundry sand (WFS-300) has a high adsorption efficiency and methylene blue adsorption follows.

Keywords: Waste foundry sand, Adsorption study, Dye removal, Methylene blue, Pollutant abatement.

INTRODUCTION

Clean and safe drinking water has emerged as a significant concern for humans, aquatic flora and fauna in recent years [1,2]. As a whole, water pollution is on the rise due to human activity, which includes technological advancements, economic growth, rising prosperity and population growth around the world [3,4]. Chemical effluents from industries and human garbage are the main sources of water contamination. Dye, metal, organic and inorganic pollutants are the most common in effluent stremes, which pose a serious threat to human health, the environment and animal life as a whole [5]. The presence of even trace amounts of dye in effluents can have a negative impact on aquatic life, including photosynthesis and visibility [5]. Other significant obstacle against humanity must overcome is the disposal of garbage from urban, rural and industrial settings [6]. The advancement and realization of affluent human lifestyles are hindered by the creation of massive amounts of trash through industrial production and scientific research and the subsequent disposal of this waste poses a threat to the environment due to pollution [7-9]. Based on the information provided, a strategy to transform foundry sand, an industrial waste product, into valuable adsorbent materials is developed [10].

Elimination of hazardous dyes from wastewater is a difficult task that presents a significant obstacle. In literature, several methods are reported like photodegradation [11], solvent extraction [12,13], adsorption [14], chemical precipitation [15], ion exchange [16], membrane filtration [17], physical adsorption [18], chemical oxidation/reduction [19,20] and bio-removal [21]. There has been a growing global interest in the sustainable methods for the removal of colours from wastewater [22,23]. The every method have its own pros and cons and as a result, researchers are scrambling to find the safest, most cost-effective way to remove toxic pollutants from effluents. Among these existing approaches, adsorption is well-known for its ease of use, simplicity, low sludge formation and great utility [24]. A wide range of adsorbent materials is utilized in adsorption procedures, encompassing both naturally occurring and labor-

atory synthesized compounds [25]. Methylene blue (MB) is a dye commonly employed for the purpose of colouring various products including as textiles, paper and leather [26]. Moreover, it is commonly employed in the field of human and veterinary medicine for many therapeutic and diagnostic uses [27]. In human body, methylene blue induces many physiological responses including increased heart rate, vomiting, shock, organ formation, cyanosis, jaundice, quadriplegia and tissue necrosis [28,29]. There is evidence indicating a correlation between it and lung and urinary bladder cancer, as well as chromosomal damage in humans [30,31]. Due to its complex aromatic constituents, hydrophilic composition, light resistance and temperature resistance, standard water treatment methods are unable to fully breakdown it [32,33]. Therefore, the urgent necessity to address the removal of toxic methylene blue dye is evident. Furthermore, the disposal of waste foundry sand (WFS) poses a significant challenge for many foundry industries. A substantial amount of this sand is disposed of in landfills, leading to soil and water pollution.

Therefore, in order to tackle this issue and establish a waste-to-useful approach in this study, the primary objective is to utilize industrial waste as adsorbent materials for water remediation. Following a minimal modification process involving the annealing of WFS at several temperatures in a muffle furnace, the resulting WFS is utilized as highly effective adsorbent materials. Furthermore, the practical findings obtained in the field strongly suggest that the WFS adsorbent can be directly utilized in large-scale wastewater treatment facilities to effectively eliminate various types of pollutants, even in challenging conditions. The primary objective of the study was to employ waste foundry sand (WFS) for efficient adsorption of methylene blue dye and investigate the sorption capabilities of modified waste foundry materials. The most common isotherms, such as Freundlich and Langmuir, were used to elucidate the mechanism of adsorption. The investigation of adsorption rate is conducted utilizing the widely employed kinetic theoretical frameworks of pseudo first order and pseudo second order kinetics. The technology of adsorption has proven to be highly effective in the removal of dyes throughout the water treatment process, owing to its user-friendly nature, exceptional efficiency and economic viability.

EXPERIMENTAL

Modification of waste foundry sand (WFS) adsorbent: Waste foundry sand (WFS) was collected from the local foundry industry Kolhapur city of India. The collected WFS were rinsed with deionized water to eliminate the colour impurities and other water soluble materials. The WFS dried in an electric oven at 110 ºC and annealed in muffle furnace at 300, 400 and 500 ºC (labelled as WFS-300, WFS-400, WFS-500). The effective adsorbent materials were stored in air tight moisture free environment and used over the experiment.

Preparation of adsorbate (MB dye) solution: Methylene blue (MB) dye solution stock solution (1000 mg L^{-1}) was prepared by dissolving a calculated amount of solid MB dye crystals in distilled water. All of the required test solutions were prepared by diluting the MB dye stock solution.

Characterization: Various techniques were used to characterize the prepared WFS materials, including X-ray diffraction analysis (XRD) (Bruker, D2-Phaser X-ray diffractometer) for structural confirmation and the nature of WFS adsorbent. Fourier Transformer Infrared spectroscopy (FTIR) (Jasco, FT IR-4600 type A, Sr. no. D044761786) was used to identify functional groups. Field Emission Scanning Electron Microscopy (FE-SEM) (Jeol-JSM-6360) was used to determine the morphology of porous surfaces and the alteration of surface roughness. To confirm the chemical states and surface chemistry of the adsorbent at room temperature, high-resolution X-ray photoelectron spectroscopy (HR-XPS, VG Multi lab 2000, Thermo VG Scientific, UK) was used. The elemental composition was determined using energy-dispersive X-ray spectroscopy (EDS, Oxford INCA system). UV-VIS spectrophotometer (EQIP-TRONICS, Digital Spectrophotometer, EQ 825) for dye concentration measurement.

Batch adsorption experiments: Batch adsorption tests were carried out by agitating a series of 250 mL Erlenmeyer flasks containing 0.3 g of WFS and 100-700 mg L^{-1} MB dye solution on a mechanical shaker for 180 min. The pH of the solution was adjusted to 9, and flasks were stirred at 150 rpm. Following equilibrium, the dye was separated using Whatman filter paper no. 41 and the concentration of unadsorbed dye was evaluated using a UV-Vis spectrophotometer. After confirming Beer-Lambert's law, the dye absorption was measured at 663 nm. Eqn. 1 was used to evaluate the amount of dye absorbed per gram.

$$q_e = \frac{C_o - C_e}{M} \times V \quad (1)$$

where q_e is the equilibrium concentration on the adsorbent, C_o and C_e (mg L^{-1}) are the initial and equilibrium concentrations of MB dye; M is the mass of adsorbent employed; and V is the volume of solution. The experimental findings were calculated in terms of the percentage elimination of MB dye. Using eqn. 2, the elimination of MB dye was calculated

$$R\ (\%) = \frac{C_o - C_e}{C_o} \times 100 \quad (2)$$

where C_o and C_e are the initial and equilibrium concentration of MB dye.

RESULTS AND DISCUSSION

XRD studies: The phase formation and crystal structure was determined by the XRD technique. Fig. 1 shows the XRD patterns of WFS annealed at different temperatures *viz*. 300, 400 and 500 ºC demonstrated well-defined diffraction peaks indicating the crystallinity is more at higher temperature [34]. The mineralogical composition WFS is of a single crystalline phase identified as quartz (SiO_2) [35]. While the adsorption efficiency of this sand decreased with increasing annealing temperature. Finally, the dye molecules may have been well distributed inside the WFS-300 micro- and macropores. The WFS-300 is more amorphous compared with others WFS-400, WFS-500 annealed sand. The XRD study revealed the change

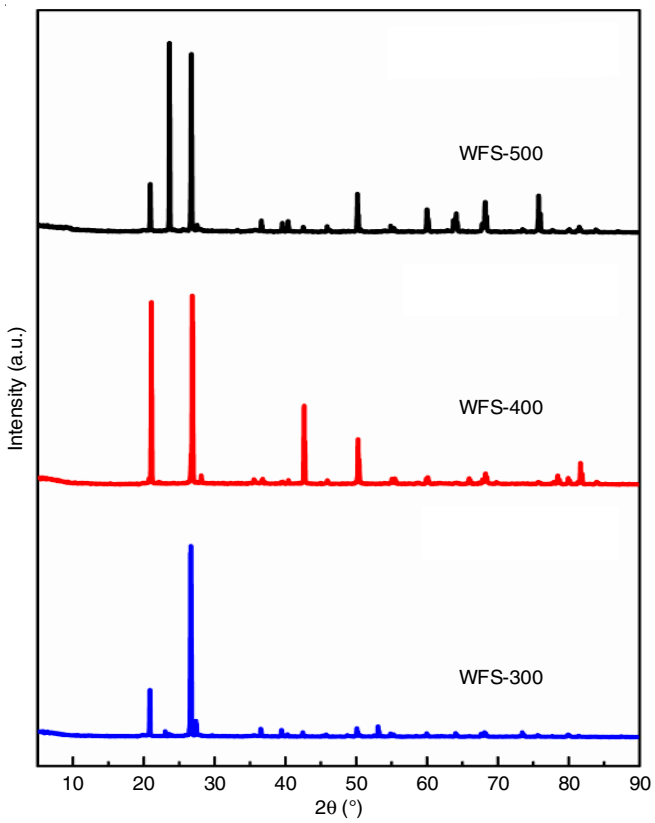

Fig. 1. XRD spectrum of annealed waste foundry sand

in crystallinity when annealed temperature increased also crystallinity increased and adsorption decreased [9].

XPS studies: Fig. 2 depicts the XPS spectrum of WFS-300, Fig. 2a shows XPS survey spectrum with presence of Si, Fe, C and O, whereas Fig. 2b illustrates the binding energies of Fe $2p_{3/2}$ and Fe $2p_{1/2}$ determined in this study [36]. The originated at binding energy 707 eV is assigned to Fe-metal while the peak at 711 eV is due to Fe^{3+} oxidation state. The absorption peak at 719 and 723 eV is due to Fe_3O_4 while the statelite peak at 716 eV assigned the presence of Fe_2O_3 [37,38]. At the outset waste foundry sand is composed Fe metal, Fe_2O_3 and Fe_3O_4 structure. Fig. 2c shows the presence of carbon in the core-level spectrum for C1 s, which contains three peaks at the binding energy. 284.5 eV corresponds to a C-C bond, 286.7 eV to a C-O-C bond and 288.9 eV to O-C=O functional groups [39]. Fig. 2d depicts a deconvoluted oxygen spectra with three peaks at binding energies of 529.6, 531.3 and 533.4 eV representing metal-oxygen, metal-carbon and C-O group, respectively [40]. The existence of silica (Si 2p) was confirmed in Fig. 2e with characteristic peak at 101.4 eV.

This represents elemental Si, surface oxide and silica. This also suggests that the waste sand containing a high ratio of surface oxides [39]. Therefore, presence of smaller micro crystalline structure causes the high surface activity, which is leading to stronger interaction between the foundry sand grains when coupling with dye molecule [35].

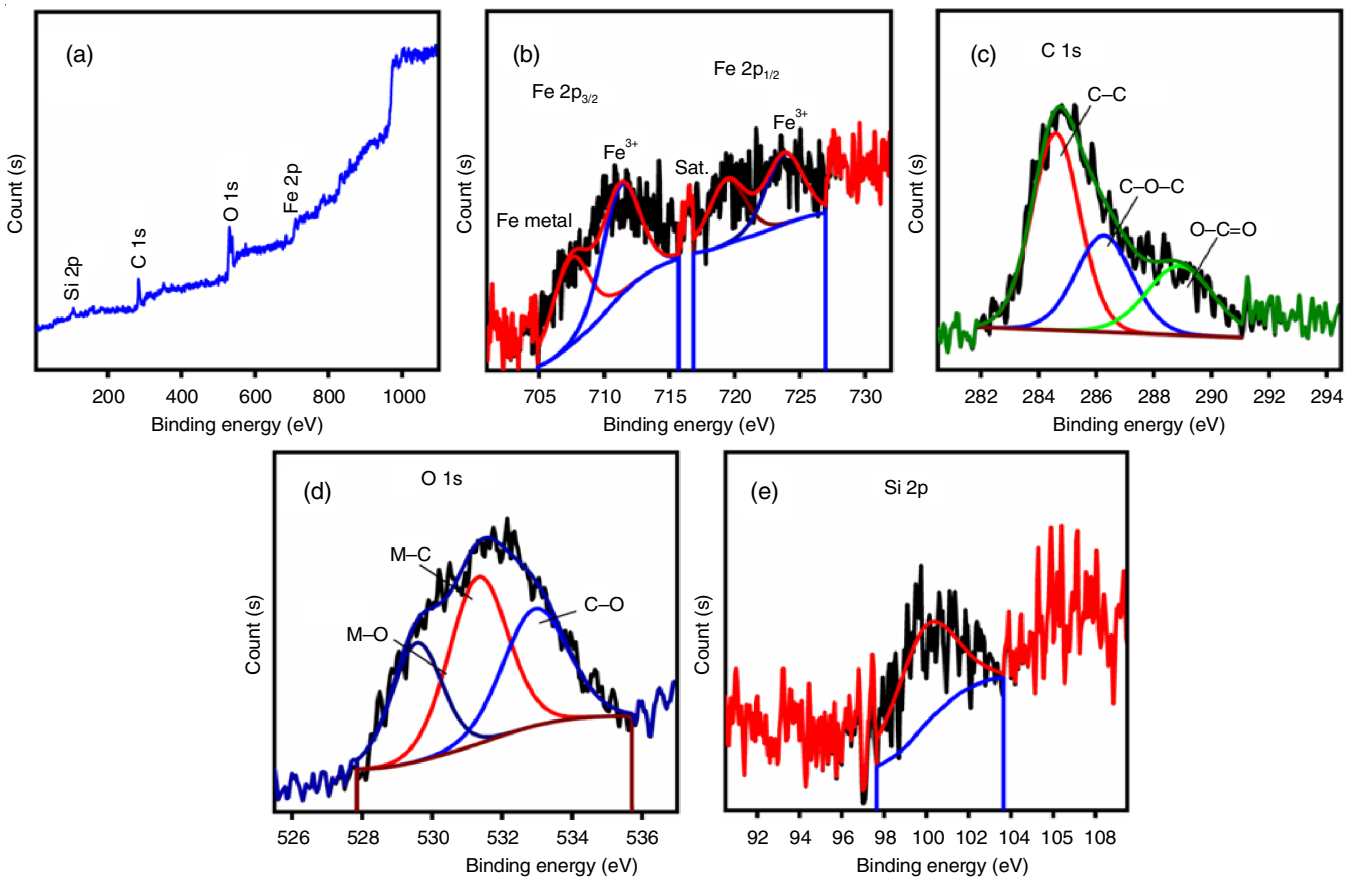

Fig. 2. (a) XPS survey spectra of WFS-300, (b) core-level spectrum of Fe 2p, (c) core-level spectrum of C1 s, (d) core-level spectrum of O1 s (e) core-level spectrum of Si 2p

FE-SEM studies: Fig. 3a-b illustrate the rough surface area of the adsorbent before adsorption, whereas Fig. 3c-d show a micrograph of WFS-300 following dye adsorption with a flat surface. The change in the surface area demonstrates that methylene blue dye was successfully adsorbed on the rough surface of the WFS-300 adsorbent.

FTIR studies: Using FTIR technique, the effective functional groups responsible for WFS sites during sorption [41,42] were analyzed. To address the decrease in transmittance for the WFS sample prior to adsorption (Fig. 4a). A spectrophotometer with infrared spectra ranging from 400 to 4000 cm^{-1} was used. The changes in the infrared frequencies of bonds (O-H band, H-O-H band, O-Si-O band and Si-O band) have wavenumbers of 3400, 1711, 1402 and 564 cm^{-1}, respectively [43].

Raman studies: The Raman spectra was used to investigate the distinct phases of WFS-300 as depicted in Fig. 4b. The band at 156, 417, 467, 666, 1005, 1113, 1609 cm^{-1} gives the characteristics of the materials in SiO_2 phase had seven major peaks that were visible in the Raman band [44].

Particle size distribution: Fig. 5 depicts the particle size distribution ranging from 353.4 to 1614.5 nm, with an average value of 984 nm. This data confirmed the classification of the waste as exhaust sand rather than exhaust dust as the latter has lesser granularity. The particle size distribution curve, waste foundry sand is effective and medium in size SiO_2, Al_2O_3 and Fe_2O_3 make up the majority of the WFS, with values of 94.36, 2.82 and 2.12%, respectively. The quantities of Na_2O and CaO in WFS are quite low, accounting for 0.24% and 0.05%, respectively.

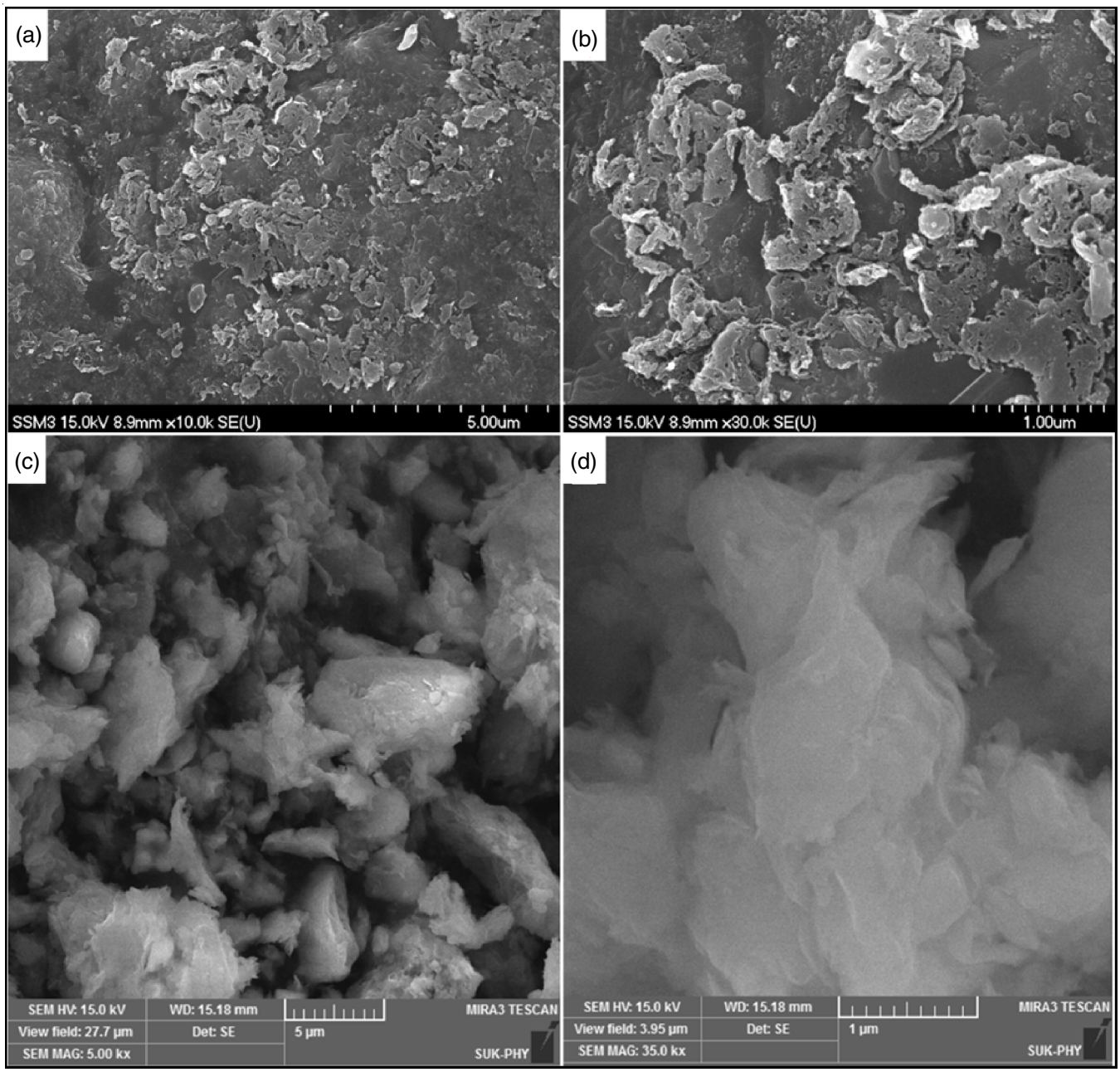

Fig. 3. SEM image of (a,b) WFS-300 adsorbent material and (c,d) is after adsorption of methylene blue dye on surface of WFS-300 sample

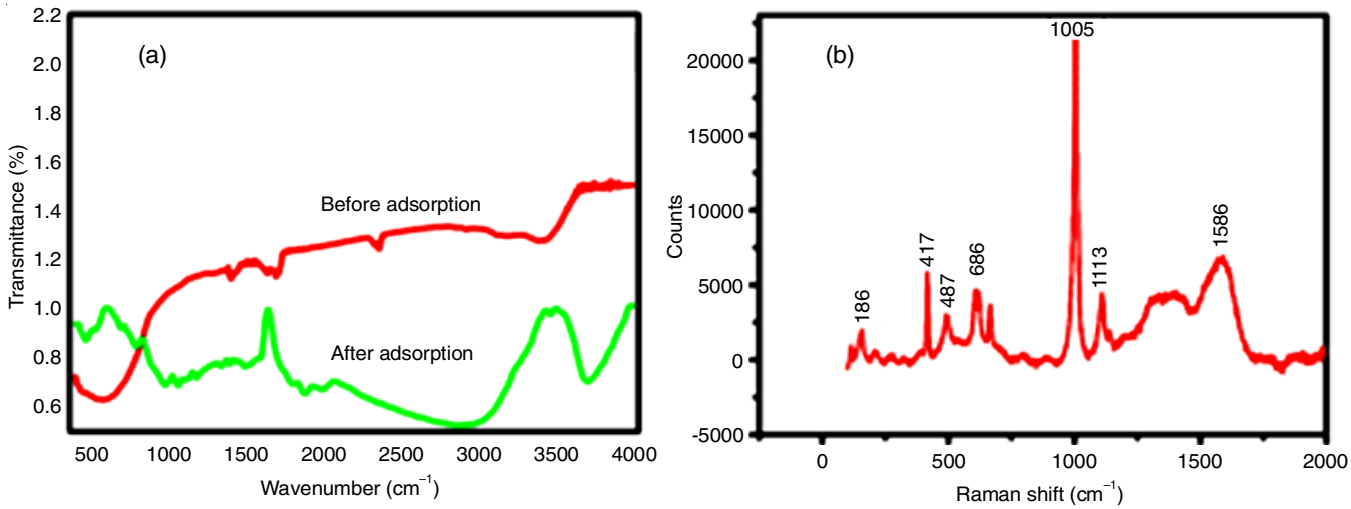

Fig. 4. (a) FTIR of after and before adsorption of methylene blue dye on WFS-300 sample and (b) Raman spectra of WFS-300 sample

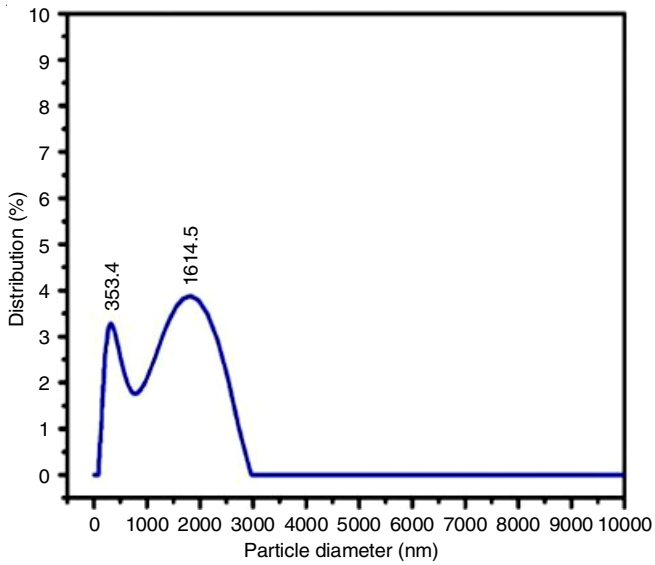

Fig. 5. Particle size distribution of WFS-300 sample

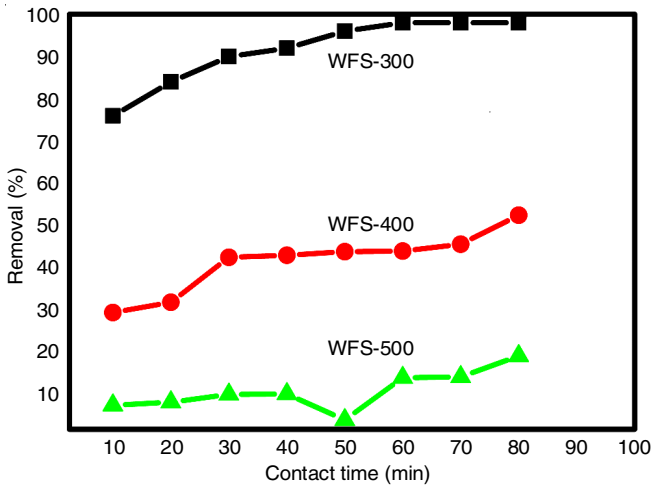

Fig. 6. Annealing effect of waste foundry sand (WFS) on methylene blue adsorption

Adsorption studies

Annealing effect of WFS on adsorption: To ensure the effectiveness of adsorption process the WFS-300, WFS-400 and WFS-500 adsorbent material were tested with methylene blue dye solutions. Three different conical flasks were used containing 0.3 g of WFS-300, WFS-400 and WFS-500, respectively. The 100 mL of dye solution with dye concentrations of 100 mg/L were added. The solution was agitated for a predetermined time period. A UV-visible spectrophotometer was used to measure the amounts of unadsorbed methylene blue dye. The percentage removal efficiency of three annealed WFS is illustrated in Fig. 6a. The results demonstrated that WFS-300 has more removal efficiency towards methylene blue dye than WFS-400 and WFS-500 adsorbent materials. Hence, it is optimized that the WFS-300 is utilized for further adsorption studies.

Effect of pH: To evaluate the effect of initial pH of the solution on adsorption process the pH of working solution was adjusted in between range 2-10 by using HCl and KOH solutions. A 100 mL of 100 mg/L dye solution containing and 0.3 g/100 mL of adsorbent were added in a conical flask. The conical flask was placed on the magnetic stirrer at room temperature and after 60 min the solution was filtered with whatmann filter paper and absorbance was recorded using a UV spectrophotometer. Fig. 7a depicted the percentage removal of methylene blue dye by employing WFS-300 adsorbent.

The results showed that when pH increased, the percentage removal of methylene blue dye increased and reached equilibrium at 98% in the presence of negatively charged groups present at the adsorbent surface for cationic dye adsorption. As a result, higher dye removal was enabled by the availability of a more negatively charged surface of adsorbent. As the pH increased, the negative charged site also increased subsequently the percentage elimination of methylene blue dye also increases [45]. A similar results are reported in literature for the pH of working solution by Patil *et al.* [46].

Effect of dosage: In a series of conical flask the WFS-300 were added as 0.05 to 0.45 g containing 100 mg/L of 100 mL methylene blue dye solution. The solution were shaked for 1 h on magnetic stirrer.The final dye concentration readings were recorded and plotted as shown in Fig. 7b. Here the amount of

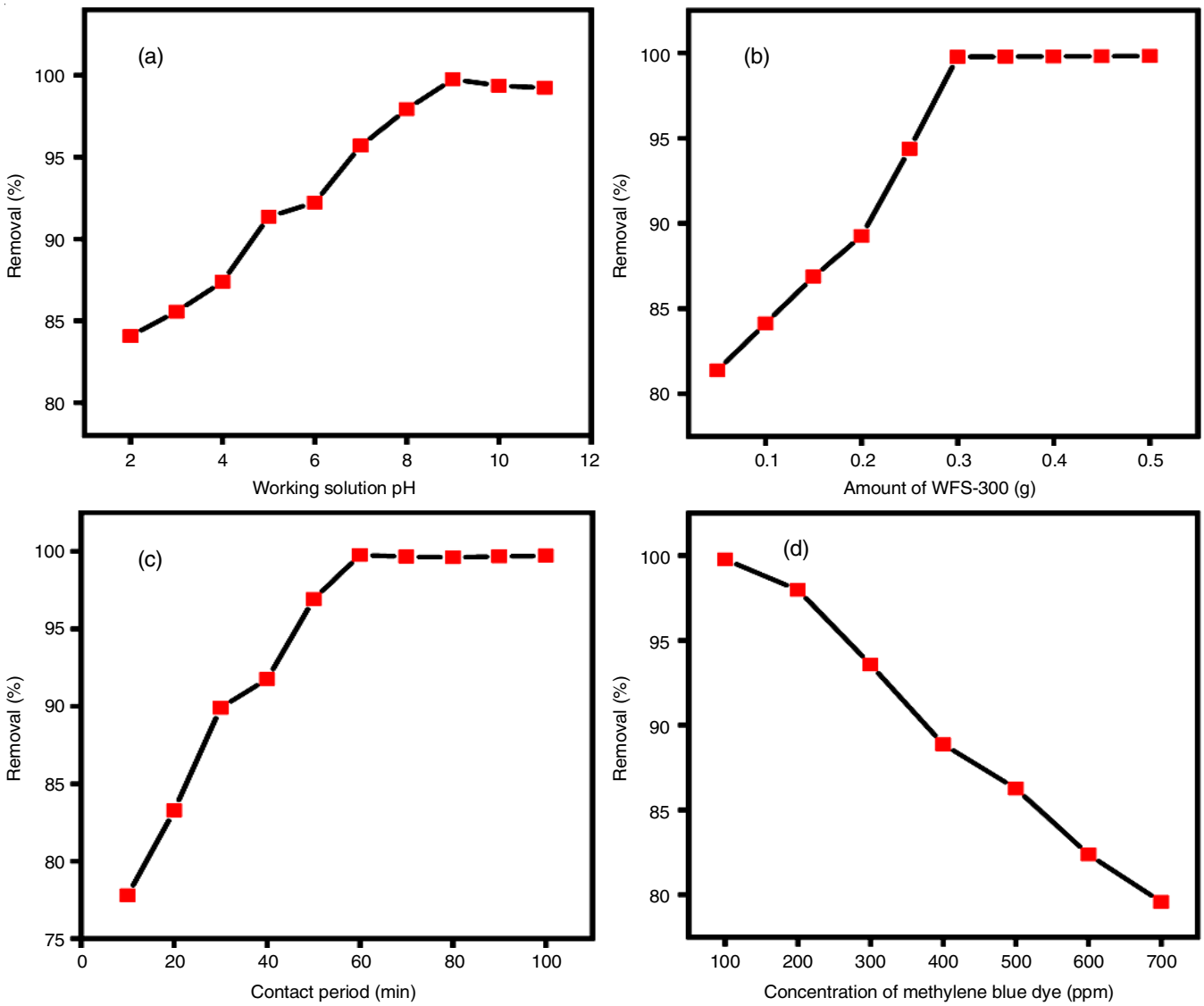

Fig. 7. (a) Effect of solution pH, (b) Effect of amount of WFS-300 adsorbent, (c) Effect of contact period, and (d) Effect of concentration of methylene blue dye on adsorption

adsorbent increases, the effective active site increases with increasing surface area and the percentage removal increases until it reaches equilibrium at 0.3 g for 98% removal, after which no further significant variations were observed.

Effect of contact period: Fig. 7c represents the graph of effect of contact period between WFS-300 and methylene blue dye. The findings indicate that there is a positive correlation between the duration of contact and the percentage of removal, with the latter reaching equilibrium within a time frame of 60 min. The uptake rate of methylene blue dye was faster in the beginning, but after equilibrium, it became constant and no significant change was observed. However, 98% of dye was successfully removed after 60 min. To determine the uptake rate of methylene blue dye, the obtained experimental data was used in the most used kinetic models such as pseudo-first order and pseudo-second order.

Pseudo-first order and pseudo-second order kinetics: The experimental data was used with a pseudo-first-order model [47] to calculate the uptake rate and the graph of log ($q_e - q_t$) against t was plotted for methylene blue dye on WFS-300 (Fig. 8a). Eqn. 3 gives the linear form of the pseudo-first order model as follows:

$$\log(q_e - q_t) = \log(q_e) - \left(\frac{k_1}{2.303}\right)t \quad (3)$$

where q_e and q_t (mg g^{-1}) represent the amount of dye adsorbed at equilibrium and time t, k_1 (min^{-1}) is rate constant. The plot of log ($q_e - q_t$) *versus* t gives values of k_1.

From the plot the adsorption capacity and constant were calculated and tabulated in Table-1. K_1 was determined from the slope and q_e was determined from the graph's intercept.

TABLE-1
KINETIC PARAMETER CONSTANT VALUE FOR ADSORPTION OF METHYLENE BLUE DYE ON WFS-300

Pseudo-first order kinetic model	q_e (mg/g)	K_1 (L/min)		R^2
	4.3853	0.0177		0.84
Pseudo-second order kinetic model	K_2	q_e	q_e^2	R^2
	6.036	9.99	99.80	0.99

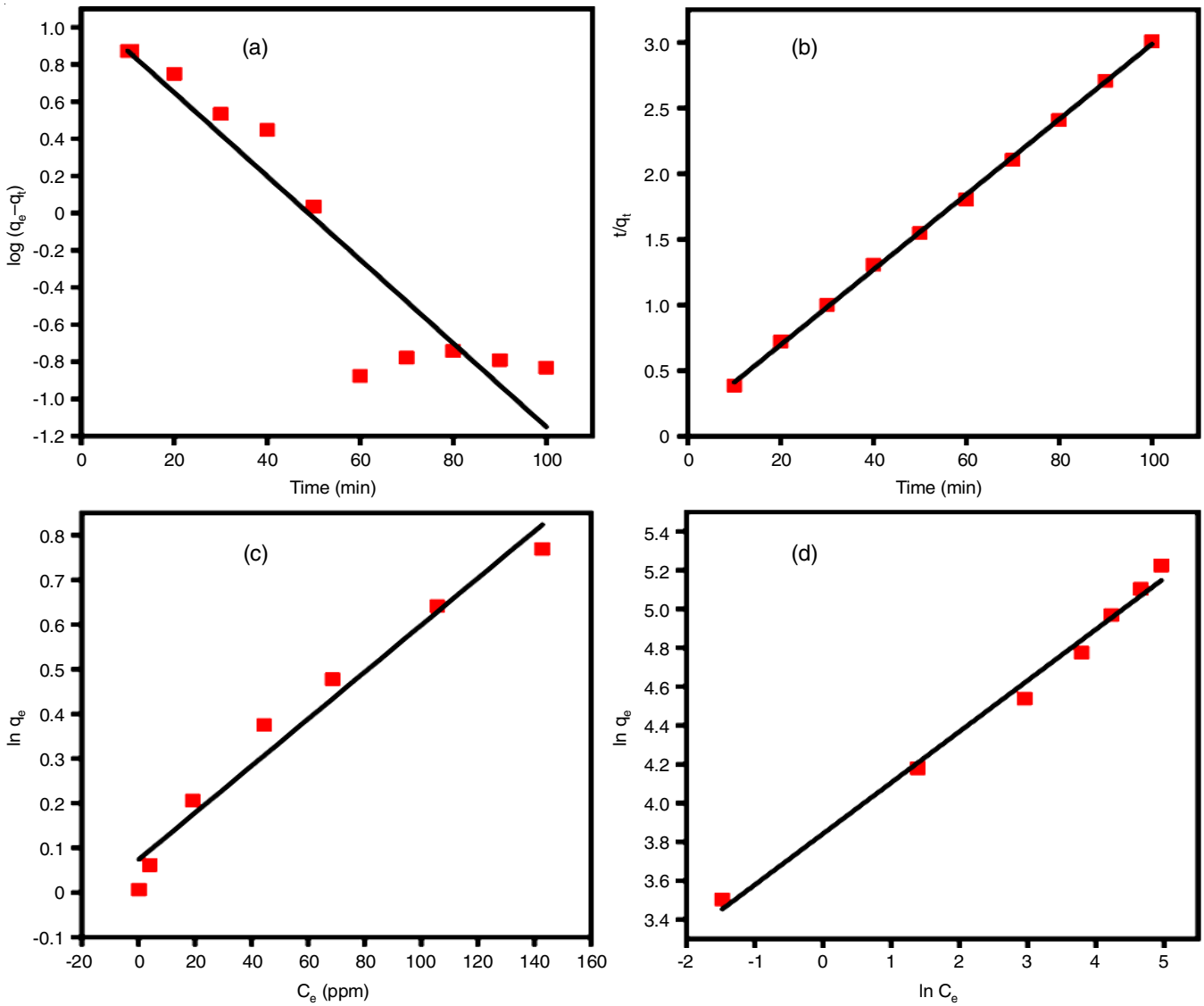

Fig. 8. (a) Pseudo-first order kinetic model, (b) Pseudo-second order kinetic model, (c) Langmuir adsorption isotherm and (d) Freundlich adsorption isotherm

The simplest linear form of pseudo-second-order kinetic model, as proposed by Ho & McKay [48], is based on the rate-limiting step of chemisorptions. The linear form is as given in eqn. 4:

$$\frac{1}{q_t} = \frac{1}{k_2 q_e^2} + \left(\frac{1}{q_e}\right) t \quad (4)$$

where q_e (mg g^{-1}) and q_t (mg g^{-1}) is equilibrium amount and time interval amount of methylene blue dye adsorbed. The k_2 (g mg^{-1} min^{-1}) is pseudo-second-order rate constant. The value of q_e and k_2 were obtained from plot of q_t *versus* t using the slope and intercept (Fig. 8b). A comparison of correlation coefficient values reveals that the pseudo-second-order kinetic model ($R^2 = 0.99$) was better suited to fitting the experimental data. Fig. 8b demonstrates that methylene blue dye adsorption on WFS-300 follows a pseudo-second-order kinetic model.

Effect of initial concentration of methylene blue dye: The dosage of methylene blue dye adsorbed per unit mass of adsorbent increased while the percentage clearance decreased as the initial concentration of methylene blue dye increased at constant room temperature for 60 min. This effect was tested at a concentration range of 100-700 mg L^{-1} while holding all other predetermined parameters constant and using 0.3 g of WFS-300 adsorbent. This batch adsorption study was run at a constant room temperature for 60 min. Fig. 8d depicts the effects of initial methylene blue dye concentration on efficient percentage removal. With increasing dye concentration, the percentage removal of methylene blue dye reduces from 98% to 91.37%. The initial concentration acts as a powerful driving force in overcoming all methylene blue dye mass transfer resistances across the aqueous and solid phases. As a result, greater mass transfer of methylene blue dye from exterior to interior was observed during this adsorption process at higher initial concentration sites [49].

Adsorption isotherm studies: The most commonly used models are the Langmuir and Freundlich isotherms. Both models were utilized in this study to explain the relationship between the amount of methylene blue dye adsorbed and its equilibrium

concentration [50,51]. This is the linear form of the Langmuir adsorption isotherm [52,53].

$$\frac{C_e}{q_e} = \frac{1}{q_m \times K_L} + \frac{C_e}{q_m} \quad (5)$$

where q_m (mg g^{-1}) is maximum adsorption capacity, K_L (L mg^{-1}) is Langmuir constant, q_e is equilibrium amount and C_e is equilibrium concentration. The parameters q_m and K_L was calculated from the plot of C_e/q_e *vs*. C_e with $1/q_m$ is slope and $1/K_L$, q_m equal to intercept [46].

Freundlich adsorption isotherm [54] based on adsorbate uptake by multilayer adsorption on heterogeneous surfaces. Freundlich's equation has a linear form:

$$\ln q_e = \ln K_F + \left(\frac{1}{n}\right) \ln C_e \quad (6)$$

where K_F (mg g^{-1}) is the Freundlich constant related to the adsorption capacity and n indicates the intensity of adsorption, q_e (mg g^{-1}) and C_e (mg L^{-1}) are amount adsorbed and equilibrium concentration of methylene blue dye.

The suitability of an isotherm corresponds with a coefficient of variation (R^2) tabulated with other parameter values in Table-2. The linear graph of both isotherms is depicted in Fig. 8c-d. The Langmuir model demonstrates better suitability (R^2 = 0.98) compared to Freundlich isotherm model ((R^2 = 0.97) as evidenced by the maximal monolayer adsorption capacity of WFS-300 at 190.47 mg g^{-1}.

TABLE-2
ISOTHERM PARAMETER CONSTANT VALUE

Langmuir model		Freundlich isotherm	
Constant	Value	Constant	Value
K_L (L mg^{-1})	0.072	K_f (L mg^{-1})	47.44
q_{max}	190.47	1/n	0.263
R^2	0.98	R^2	0.97

Recyclability study: The ability of annealed WFS-300 as an adsorbent to regenerate and maintain performance during the adsorption process is the two key factors that determine its practical application. The sorbent employed in this study for the removal of methylene blue dye molecules and subsequent regeneration of the used sorbent was subjected to tests to assess its recyclability [55,56]. The results of five times recycling are shown in Fig. 9 and the sorbent can be utilized again. The comparisons of efficiency of the adsorption capacity with other adsorbent materials is tabulated in Table-3.

Conclusion

Waste foundry sand (WFS) was successfully modified at 300 ºC and utilized as adsorbent materials for adsorption of methylene blue dye. The comparative XRD spectra shows a good crystalline nature of WFS and WFS-300 showed excellent response for removing the methylene blue dye compared to other WFS-400 and WFS-500. The maximum 98% methylene blue dye were adsorbed at optimized pH-8, within 60 min at 0.3 g WFS-300 adsorbent dosage. The results were matched with the well-known Langmuir adsorption isotherm, with a maximum monolayer adsorption capacity of 190.47 mg/g. The uptake rate of methylene blue dye on WFS-300 follows a pseudo-second order kinetic model. These findings indicated that a waste-to-use methodology can be applied to efficiently utilize the waste foundry sand as an absorbent for methylene blue dye.

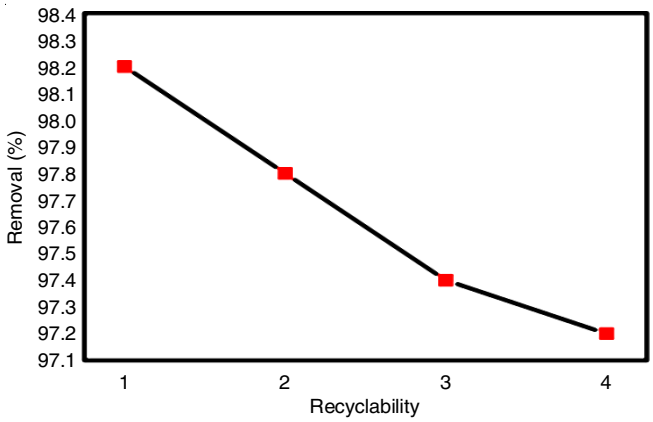

Fig. 9. Recyclability test of WFS-300 adsorbent

TABLE-3
COMPARISON OF THE ADSORPTION CAPACITY OF WFS-300 IN COMPARISON WITH OTHER ADSORBENTS

Adsorbent	Adsorption capacity	Ref.
Cobalt-zinc ferrite	32.30 mg/g	[57]
WFS/Cu(II)	7.153 mg/g	[58]
Lignocellulosic agriculture waste	148.8 mg/g	[55]
AC500/NZ	51 mg/g	[56]
Twigs-derived activated carbons	217 mg/g	[59]
Graphene Oxide	1.939 mg/mg	[60]
Spent rice biomass (SRB)	8.13 mg/g	[61]
Soursop	55.39 mg/g	[62]
Sugarcane bagasse	17.43 mg/g	[62]
WFS-300	190.47 mg/g	Present work

CONFLICT OF INTEREST

The authors declare that there is no conflict of interests regarding the publication of this article.

REFERENCES

1. X. Lei, Q. Lian, X. Zhang, T.K. Karsili, W. Holmes, Y. Chen, M.E. Zappi and D.D. Gang, *Environ. Pollut.*, **321**, 121138 (2023); https://doi.org/10.1016/j.envpol.2023.121138
2. N.F. Carrard, T. Foster and J. Willetts, *Water*, **11**, 1605 (2019); https://doi.org/10.3390/w11081605
3. P. Ekins and D. Zenghelis, *Sustain. Sci.*, **16**, 949 (2021); https://doi.org/10.1007/s11625-021-00910-5
4. X. Tian, Population Quality and Sustainable Development, In: An Essay on China's Development After the Demographic Golden Age, Springer Nature Singapore, Singapore, pp. 201-225 (2023).
5. J. Lin, W. Ye, M. Xie, D.H. Seo, J. Luo, Y. Wan and B. Van der Bruggen, *Nat. Rev. Earth Environ.*, **4**, 785 (2023); https://doi.org/10.1038/s43017-023-00489-8
6. R. Siddique, G. Kaur and A. Rajor, *Resour. Conserv. Recycling*, **54**, 1027 (2010); https://doi.org/10.1016/j.resconrec.2010.04.006
7. P. Shikalgar, P. Ghatge, P. Kumbhar, S. Patil, S. Kolekar and A. Sartape, *Bull. Environ. Pharmacol. Life Sci.*, **3**, 189 (2021).
8. A. Štrkalj, Z. Glavaš and I. Brnardic, *Chem. Biochem. Eng. Q.*, **27**, 15 (2013).
9. P.M. Sundari, T. Santhi and T. Meenambal, *Asian J. Chem.*, **25**, 4434 (2013); https://doi.org/10.14233/ajchem.2013.14010

10. S. Rha and H.Y. Jo, *J. Hazard. Mater.*, **412**, 125290 (2021); https://doi.org/10.1016/j.jhazmat.2021.125290
11. R. Ghaware, P. Sanadi, D. Narale, R. Bhosale, K. Patil, J.H. Kim and S. Kolekar, *ChemistrySelect*, **8**, e202301320 (2023); https://doi.org/10.1002/slct.202301320
12. E.S.Z. El-Ashtoukhy and Y.O. Fouad, *Alex. Eng. J.*, **54**, 77 (2015); https://doi.org/10.1016/j.aej.2014.11.007
13. G.D. Kore, S.A. Patil, M.A. Anuse and S.S. Kolekar, *J. Radioanal. Nucl. Chem.*, **310**, 329 (2016); https://doi.org/10.1007/s10967-016-4857-7
14. S.A. Patil, P.D. Kumbhar, B.S. Satvekar, N.S. Harale, S.C. Bhise, S.K. Patil, A.S. Sartape, S.S. Kolekar and M.A. Anuse, *J. Iran. Chem. Soc.*, **19**, 2891 (2022); https://doi.org/10.1007/s13738-022-02500-3
15. Z. Yang, M. Li, M. Yu, J. Huang, H. Xu, Y. Zhou, P. Song and R. Xu, *Chem. Eng. J.*, **303**, 1 (2016); https://doi.org/10.1016/j.cej.2016.05.101
16. M.S. Mohy Eldin, M.H. Gouda, M.A. Abu-Saied, Y.M.S. El-Shazly and H.A. Farag, *Desalination Water Treat.*, **57**, 22049 (2016); https://doi.org/10.1080/19443994.2015.1128363
17. M. Shamim Sheikh, M. Mahmudur Rahman, M. Safiur Rahman, K. Yildirim and M. Maniruzzaman, *J. Ind. Eng. Chem.*, **128**, 196 (2023); https://doi.org/10.1016/j.jiec.2023.07.048
18. P.P. Bote, S.R. Vaze, C.S. Patil, S.A. Patil, G.B. Kolekar, M.D. Kurkuri and A.H. Gore, *Environ. Technol. Innov.*, **24**, 102047 (2021); https://doi.org/10.1016/j.eti.2021.102047
19. R. Begum, J. Najeeb, A. Sattar, K. Naseem, A. Irfan, A.G. Al-Sehemi and Z.H. Farooqi, *Rev. Chem. Eng.*, **36**, 749 (2020); https://doi.org/10.1515/revce-2018-0047
20. K. Dutta, S. Mukhopadhyay, S. Bhattacharjee and B. Chaudhuri, *J. Hazard. Mater.*, **84**, 57 (2001); https://doi.org/10.1016/S0304-3894(01)00202-3
21. R.G. Saratale, G.D. Saratale, J.S. Chang and S.P. Govindwar, *Biodegradation*, **21**, 999 (2010); https://doi.org/10.1007/s10532-010-9360-1
22. U. Ewuzie, O.D. Saliu, K. Dulta, S. Ogunniyi, A.O. Bajeh, K.O. Iwuozor and J.O. Ighalo, *J. Water Process Eng.*, **50**, 103273 (2022); https://doi.org/10.1016/j.jwpe.2022.103273
23. G.A. Ismail and H. Sakai, *Chemosphere*, **291**, 132906 (2022); https://doi.org/10.1016/j.chemosphere.2021.132906
24. S.A. Patil, U.P. Suryawanshi, N.S. Harale, S.K. Patil, M.M. Vadiyar, M.N. Luwang, M.A. Anuse, J.H. Kim and S.S. Kolekar, *Int. J. Environ. Anal. Chem.*, **102**, 8270 (2022); https://doi.org/10.1080/03067319.2020.1849648
25. C. Valli Nachiyar, A.D. Rakshi, S. Sandhya, N. Britlin Deva Jebasta and J. Nellore, *Case Stud. Chem. Environ. Eng.*, **7**, 100339 (2023); https://doi.org/10.1016/j.cscee.2023.100339
26. M. Rafatullah, O. Sulaiman, R. Hashim and A. Ahmad, *J. Hazard. Mater.*, **177**, 70 (2010); https://doi.org/10.1016/j.jhazmat.2009.12.047
27. E. Rápó and S. Tonk, *Molecules*, **26**, 5419 (2021); https://doi.org/10.3390/molecules26175419
28. B.H. Hameed, A.L. Ahmad and K.N.A. Latiff, *Dyes Pigments*, **75**, 143 (2007); https://doi.org/10.1016/j.dyepig.2006.05.039
29. P.O. Oladoye, T.O. Ajiboye, E.O. Omotola and O.J. Oyewola, *Results Eng.*, **16**, 100678 (2022); https://doi.org/10.1016/j.rineng.2022.100678
30. A.S. Sartape, S.A. Patil, S.K. Patil, S.T. Salunkhe and S.S. Kolekar, *Desalination Water Treat.*, **53**, 99 (2015); https://doi.org/10.1080/19443994.2013.839404
31. A.K. Moorthy, B. Govindarajan Rathi, S.P. Shukla, K. Kumar and V. Shree Bharti, *Environ. Toxicol. Pharmacol.*, **82**, 103552 (2021); https://doi.org/10.1016/j.etap.2020.103552
32. M. Patel, R. Kumar, K. Kishor, T. Mlsna, C.U. Pittman Jr. and D. Mohan, *Chem. Rev.*, **119**, 3510 (2019); https://doi.org/10.1021/acs.chemrev.8b00299
33. G. Sharma, A. Kumar, M. Naushad, A. Kumar, A.H. Al-Muhtaseb, P. Dhiman, A.A. Ghfar, F.J. Stadler and M.R. Khan, *J. Clean. Prod.*, **172**, 2919 (2018); https://doi.org/10.1016/j.jclepro.2017.11.122
34. X. Ma, D. Xu, Y. Li, Z. Ou and A. Howard, *J. Clean. Prod.*, **349**, 131488 (2022); https://doi.org/10.1016/j.jclepro.2022.131488
35. M.A.B. Martins, L.R.R. da Silva, M.G.A. Ranieri, R.M. Barros, V.C. dos Santos, P.C. Gonçalves, M.R.B. Rodrigues, R.C.C. Lintz, L.A. Gachet, C.B. Martinez and M.L.N.M. Melo, *Materials*, **14**, 5629 (2021); https://doi.org/10.3390/ma14195629
36. S.A. Patil, P.D. Kumbhar, S.K. Patil, M.M. Vadiyar, U.P. Suryawanshi, C.L. Jambhale, M.A. Anuse, J.H. Kim and S.S. Kolekar, *Int. J. Environ. Anal. Chem.*, **102**, 1205 (2022); https://doi.org/10.1080/03067319.2020.1734197
37. H. Kim, O. Purev, E. Myung, N. Choi and K. Cho, *Int. J. Environ. Res. Public Health*, **19**, 9030 (2022); https://doi.org/10.3390/ijerph19159030
38. T. Yamashita and P. Hayes, *Appl. Surf. Sci.*, **254**, 2441 (2008); https://doi.org/10.1016/j.apsusc.2007.09.063
39. S. Kumar, R. Prakash, R. Choudhary and D. Phase, *Mater. Res. Bull.*, **70**, 392 (2015); https://doi.org/10.1016/j.materresbull.2015.05.007
40. S.A. Mane, A.V. Moholkar and A.V. Ghule, *Next Materials*, **1**, 100045 (2023); https://doi.org/10.1016/j.nxmate.2023.100045
41. C. Wang, Z. Feng and X. Wang, *Adsorpt. Sci. Technol.*, **2021**, 3820762 (2021); https://doi.org/10.1155/2021/3820762
42. D.N. Ahmed, L.A. Naji, A.A.H. Faisal, N. Al-Ansari and M. Naushad, *Sci. Rep.*, **10**, 2042 (2020); https://doi.org/10.1038/s41598-020-58866-y
43. P. Okoczuk, M. Lapiński, T. Miruszewski, P. Kupracz and L. Wicikowski, *Materials*, **14**, 2158 (2021); https://doi.org/10.3390/ma14092158
44. P. Borowicz, A. Taube, W. Rzodkiewicz, M. Latek and S. Giera³towska, *Scientific World J.*, **2013**, 208081 (2013); https://doi.org/10.1155/2013/208081
45. D. Pathania, S. Sharma and P. Singh, *Arab. J. Chem.*, **10**, S1445 (2017); https://doi.org/10.1016/j.arabjc.2013.04.021
46. S.A. Patil, S.K. Patil, A.S. Sartape, S.C. Bhise, M.M. Vadiyar, M.A. Anuse and S.S. Kolekar, *Sep. Sci. Technol.*, **55**, 2904 (2020); https://doi.org/10.1080/01496395.2019.1659366
47. H. Yuh-Shan, *Scientometrics*, **59**, 171 (2004); https://doi.org/10.1023/B:SCIE.0000013305.99473.cf
48. Y.S. Ho and G. McKay, *Process Biochem.*, **34**, 451 (1999); https://doi.org/10.1016/S0032-9592(98)00112-5
49. P. Kumbhar, S. Patil, D. Narale, A. Sartape, C. Jambhale, J.-H. Kim and S. Kolekar, *Biomass Convers. Biorefin.*, (2022); https://doi.org/10.1007/s13399-022-02625-8
50. N. Ayawei, A.N. Ebelegi and D. Wankasi, *J. Chem.*, **2017**, 3039817 (2017); https://doi.org/10.1155/2017/3039817
51. M. Belhachemi and F. Addoun, *Appl. Water Sci.*, **1**, 111 (2011); https://doi.org/10.1007/s13201-011-0014-1
52. I. Langmuir, *J. Am. Chem. Soc.*, **38**, 2221 (1916); https://doi.org/10.1021/ja02268a002
53. I. Langmuir, *J. Am. Chem. Soc.*, **39**, 1848 (1917); https://doi.org/10.1021/ja02254a006
54. H. Freundlich, *Z. Phys. Chem.*, **57U**, 385 (1907); https://doi.org/10.1515/zpch-1907-5723
55. H.M. El-Bery, M. Saleh, R.A. El-Gendy, M.R. Saleh and S.M. Thabet, *Sci. Rep.*, **12**, 5499 (2022); https://doi.org/10.1038/s41598-022-09475-4
56. F. Mohamed, M. Shaban, S.K. Zaki, M.S. Abd-Elsamie, R. Sayed, M. Zayed, N. Khalid, S. Saad, S. Omar, A.M. Ahmed, A. Gerges, H.R.A. El-Mageed and N.K. Soliman, *Sci. Rep.*, **12**, 18031 (2022); https://doi.org/10.1038/s41598-022-22421-8
57. T. Tatarchuk, N. Paliychuk, R. Babu Bitra, A. Shyichuk, M. Naushad, I. Mironyuk and D. Ziolkovska, *Water Treat.*, **150**, 374 (2019); https://doi.org/10.5004/dwt.2019.23751
58. A. Strkalj, Z. Glavas and L. Slokar, *Arch. Metall. Mater.*, **61**, 1805 (2016); https://doi.org/10.1515/amm-2016-0292
59. M.H.M. Zubir and M.A.A. Zaini, *Sci. Rep.*, **10**, 14050 (2020); https://doi.org/10.1038/s41598-020-71034-6
60. W. Zhang, C. Zhou, W. Zhou, A. Lei, Q. Zhang, Q. Wan and B. Zou, *Bull. Environ. Contam. Toxicol.*, **87**, 86 (2011); https://doi.org/10.1007/s00128-011-0304-1
61. M.S.U. Rehman, I. Kim and J.-I. Han, *Carbohydr. Polym.*, **90**, 1314 (2012); https://doi.org/10.1016/j.carbpol.2012.06.078
62. L. Meili, P.V.S. Lins, M.T. Costa, R.L. Almeida, A.K.S. Abud, J.I. Soletti, G.L. Dotto, E.H. Tanabe, L. Sellaoui, S.H.V. Carvalho and A. Erto, *Prog. Biophys. Mol. Biol.*, **141**, 60 (2019); https://doi.org/10.1016/j.pbiomolbio.2018.07.011